scientific reports

Check for updates

OPEN

Transgenic zebrafish embryos to evaluate the in vivo effects of different liposome-paclitaxel nanocarrier system

Andrea Persico[1], Laura Molteni[2], Paride Mantecca[1], Marcelo Kravicz[3,4] & Cinzia Bragato[1,4]✉

Zebrafish is an established valuable model for understanding the complex in vivo behavior of systemic nanocarrier strategies, their safety profile, and the array of possible compositions. To date, we have explored the possibility of Paclitaxel (PTX) delivery using liposome systems as a promising approach to treating cancer. Despite its benefits, this efficacious anti-cancer drug presents a main adverse effect, such as the onset of chemotherapy-induced peripheral neuropathy (CIPN). Thus, many research efforts are aimed at searching for the resolution or reduction of such problems. Taking advantage of zebrafish embryos, a powerful model for predicting and translating what is observed in humans, we investigated the plain PTX outcomes and compared them to the effects of different liposomes loaded with PTX. Since approximately 70% of human genes have at least one orthologue in zebrafish, studying the molecular mechanisms underlying chemotherapy-induced toxicity and increased oxidative stress becomes easy. First, we used a transgenic model to evaluate the systemic response to different concentrations of PTX, planning the final concentration to be loaded in liposomes, with and without functionalization. Then, we assessed the effects of this promising nanocarrier system at a molecular, histochemical, and behavioral level in reducing the detrimental side effects of the most successful cancer drug.

Keywords Transgenic zebrafish embryos, Liposome nanocarrier system, Paclitaxel, Therapeutic strategy

In the last decade, the Teleostei zebrafish (*Danio rerio*) has become one of the most widely used vertebrate models by researchers worldwide. This little fish has numerous advantages, being prolific and easy to manipulate, characterized by external fertilization and transparent offspring. One of the most attractive characteristics is that zebrafish can be a robust predictive model for different human diseases. About 80% of human disease-causing genes are conserved in this model, making the probability of identifying molecular factors with analogous functions in humans very high.

Two different populations of somatosensory neurons are present in zebrafish, called trigeminal neurons and Rohon-Beard (RB) neurons, both formed around 18 h post-fertilization (hpf) in the head and body.

The peculiarity of RB neurons is that they are transient, being present between 2 and 4 weeks of age and successively replaced by the Dorsal Root Ganglia (DRG) neurons[1,2], even if a recent research work stated that RBs do not die during early zebrafish development, surviving long past DRG formation and integration[3].

Juvenile and adult zebrafish have trigeminal and DRG neurons that are comparable to mammals. Nonetheless, RB neurons are molecularly equivalent to trigeminal and DRG neurons, sharing with them molecular markers[4,5]. Moreover, the RB neurons axons arborize within the skin as mammalian somatosensory neurons[6,7]. In the case of embryonic and larval zebrafish, RB neurons coexist with the rudimental skin, formed by two layers, the outer enveloping and the inner basal keratinocyte layer, respectively. Like mammals, the basal keratinocyte layer is innervated by unmyelinated sensory neurons. At 4 weeks developmental stage, the skin differentiates into stratified epithelium, and the DRG neurons become completely functional[8,9].

Since the beginning of the twenty-first century, zebrafish have been widely used as a model for drug discovery, given the ease of administration that can be achieved by different roots, through the aqueous environment or through injection, and the medication efficacy, bioavailability, and toxicity that can be readily determined.

[1]POLARIS Research Center, Department of Earth and Environmental Sciences, University of Milano-Bicocca, 20126 Milan, Italy. [2]Experimental Neurology Unit, School of Medicine and Surgery, University of Milano-Bicocca, 20900 Monza, Italy. [3]School of Medicine and Surgery, University of Milano-Bicocca, 20900 Monza, Italy. [4]Marcelo Kravicz and Cinzia Bragato Co-last authors. ✉email: cinzia.bragato@unimib.it

Nevertheless, the potential of lipid-based delivery systems and their versatile payload are of great interest as proper nanocarriers, providing stability, compatibility, and a reduced immune response[10].

Given the morphology similarity to cell membranes, liposomes are an optimal drug delivery system widely studied in recent 50 years and are recognized as the most successful nanocarrier system. They are used with the intent to overcome the circulation half-life of drugs, the uncontrolled biodistribution and the undesirable side effects. Furthermore, liposomes can be functionalized to increase the target tissue selectivity and have been used in efficient cancer chemotherapy regimens to incorporate and deliver a drug to the disease site. In this research work, we used a cationic liposome formulation with 1,2-Dioleoyl-3-trimethylammonium-propane (DOTAP), a positively charged lipid commonly used in the formulation of cationic liposomes, and the neutral DOPC (1,2-dioleoyl-sn-glycero-3-phosphatidylcholine) loaded with PTX. These cationic liposomes can be used for encapsulating and delivering hydrophobic drugs such as Paclitaxel (PTX) within the lipid bilayer membrane[11].

PTX, initially known as Taxol, is a taxane diterpenoid, a natural compound extracted from the Pacific yew tree, *Taxus brevifolia*. It was discovered by the National Cancer Institute (NCI) in the late 1960s during studies conducted on plant extracts searching for potential anti-cancer agents. PTX is characterized by distinctive cytotoxic properties against cancer cells, with the ability to inhibit microtubule depolymerization, leading to cell cycle arrest and apoptosis[12]. It is one of the effective antitumor agents against advanced and early-stage cancers, such as breast cancer[13], despite it being known to cause damage in healthy cells[14].

Therefore, researchers have tried to find a solution to reduce the detrimental secondary effects caused by this effective chemotherapeutic agent[15], such as chemotherapy-induced peripheral neuropathy (CIPN). This secondary effect is a sensory neuropathy that may occur as a side effect of PTX, along with motor and autonomic changes of different intensity and duration[16].

Besides CIPN, the microtubule-stabilizing PTX causes different pathological insults directly to sensory neurons, particularly at the dorsal root ganglion (DRG) level, resulting in damaged peripheral nerves and sensory axonal neuropathy development[17]. For these reasons, we decided to generate liposomes morphologically adapted to target and deliver drugs to be employed as nanocarriers precisely[18] and to test their effects in vivo using zebrafish embryos as a model.

Here, we developed liposomes functionalized with a matrix metalloproteinase (MMP) sensitive lipopeptide, here called MSLP-Lip, to deliver and release their cargo in response to the metalloproteinases (MMPs) presence[19]. Among MMPs, MMP-2 and MMP-9 are particularly increased in different tumor microenvironments[20,21]. MSLP-Lip was loaded with PTX, which is encapsulated in the liposome bilayers, thus allowing the PTX to be carried and specifically released in the target site. To evaluate PTX efficacy at toxicological, molecular, behavioral and microscopy level, we injected zebrafish embryos at 48 hpf with (i) 30 µM PTX; (ii) Liposomes loaded with 30 µM PTX (LipoPTX); (iii) Liposomes unloaded (Lipo unloaded); (iv) MSLP Liposomes loaded with 30 µM PTX (MSLP-LipoPTX); (v) MSLP Liposomes unloaded (MSLP-Lipo unloaded), compared with (vi) Ctrl not injected.

Zebrafish is an excellent model for in vivo imaging, allowing the live imaging of axon degeneration. Furthermore, the peripheral neurons development is rapid, and their differentiation occurs within 48 h, allowing CIPN evaluation in a short time[9].

Considering such a model, our research aims to evaluate the effects of these new bio-based nanocarriers and compare them with PTX in a biological milieu. A specific transgenic zebrafish line, *Tg(isl2b:GFP)*^{zb7}, was used for this purpose since it allows the visualization of somatosensory neurons under a fluorescent microscope. This preparatory work is needed to assess liposome behavior in a zebrafish xenograft model established using human breast cancer cells. We believe these efforts are necessary to set new standards in generating novel and safe therapeutic approaches to reduce the adverse consequences of the most used anti-cancer drug.

Results

Setting up the PTX concentration

We injected at 48 hpf the Tg(*isl2b*:GFP)^{zb7} embryos with PTX at a concentration of 60 nM, 100 nM, 10 µM and 22 µM in 1 nanoliter (nL) of sterile water (Supplementary Fig. 1). The experimental groups observed were (i) Ctrl not injected (n = 13); (ii) Embryos injected with PTX 60 nM, (iii) Embryos injected with PTX 100 nM, (iv) Embryos injected with PTX 10 µM, and (v) Embryos injected with PTX 22 µM.

We observed n = 39 embryos for each experimental group during three different experiments, for a total of 195 embryos observed. The results showed low mortality (less than 5%, taking into consideration the mortality on control embryos) and a negligible number of embryos presenting sublethal defects (less than 0,7% of embryos presenting cardiac edemas) (Fig. 1a, b). Furthermore, the fluorescence was observed in injected embryos' caudal fin at 48 h post injection (hpi), as a readout of peripheral sensory neurons suffering from PTX administration (Fig. 1c–e), observing no statistically significant results.

Liposomes loaded with different PTX concentrations

Based on the results obtained so far, we decided to load liposomes with PTX 30 µM and 100 µM, comparing them with PTX alone and with liposome unloaded (Lipo unloaded), at liposome concentration equivalent to LipoPTX 30 µM (A) or 100 µM (B). The following experimental groups were compared. (i) Ctrl not injected; (ii) Embryos injected with PTX 30 µM; (iii) Embryos injected with LipoPTX 30 µM; (iv) Embryos injected with Lipo unloaded A; (v) Embryos injected with PTX 100 µM; (vi) Embryos injected with LipoPTX 100 µM; and (vii) Embryos injected with Lipo unloaded B. We achieved 3 independent experiments, observing n = 32 embryos for each experimental group. We observed a high mortality percentage (40%) in embryos injected with PTX 30 µM, clearly reduced in embryos injected with LipoPTX 30 µM (12%). The same was observed in embryos injected with PTX 100 µM (31.6% of mortality), compared to embryos injected with LipoPTX 100 µM (14.6%) (Fig. 2a).

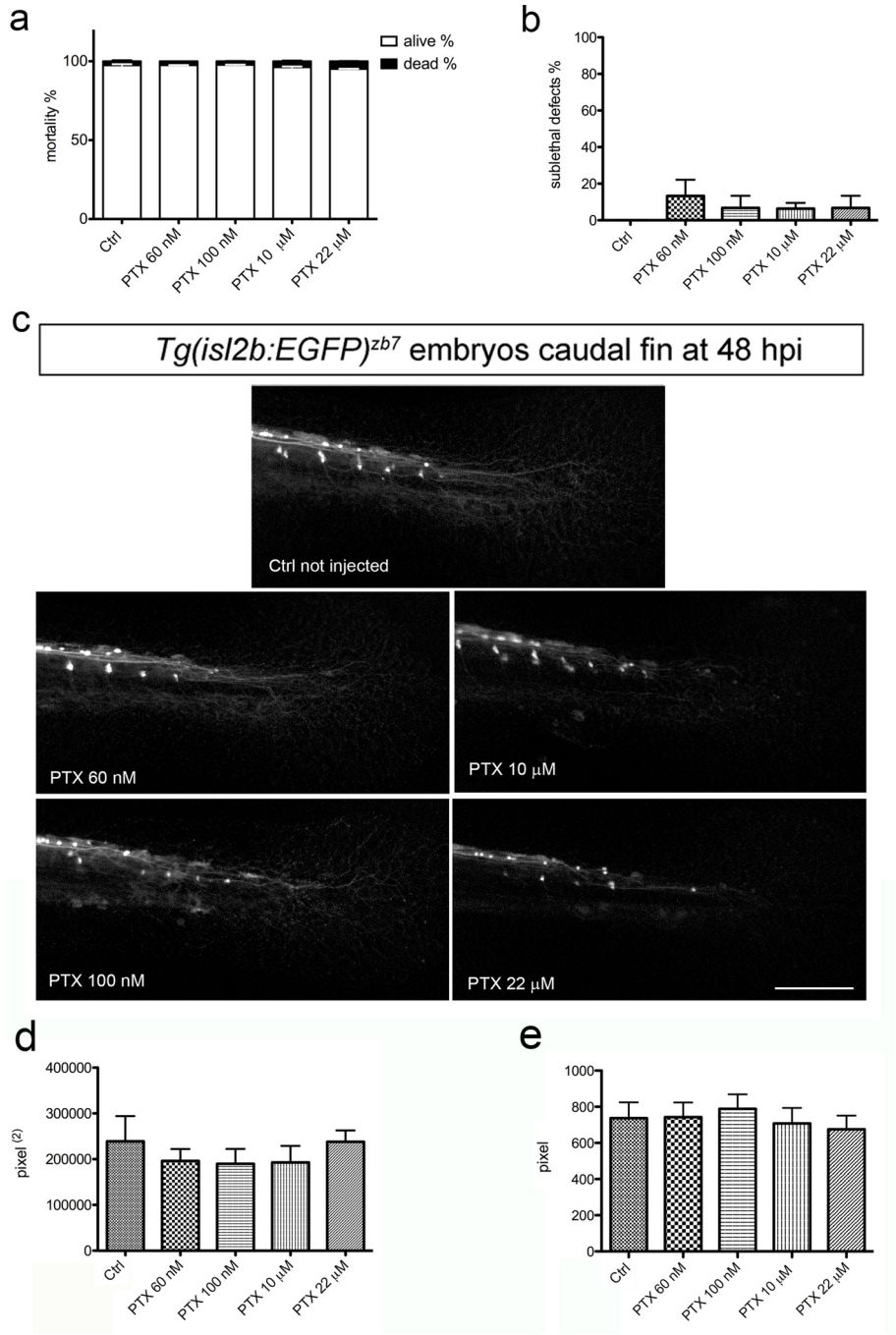

Fig. 1. Evaluation of different PTX concentrations injected in zebrafish embryos. (**a**) mortality reported in the graph showed a negligible percentage of dead embryos injected at 48 hpf, even with higher PTX concentration (22 µM). (**b**) sublethal defects average reported is less than 0.5%. The main defect observed in injected embryos is cardiac edema. (**c**) Representative images of embryos at 48 h post injection showed the frame used to analyze the GFP signal. (Scale bar, 100 µm). (**d**) graph reporting the fluorescent area measured in arbitrary units. (**e**) peripheral sensory neurons length measured and reported in graph. The effects of the different PTX concentrations were observed in n = 39 embryos for each experimental group during three different experiments, for a total of n = 195 embryos.

The average percentage of embryos alive at 48 hpi, corresponding to 96 hpf developmental stage, showed a significant decrease in living embryos after PTX 30 µM injection compared to Ctrl ($^{***}p < 0.0001$, Chi-square value = 51.57, df = 1), to LipoPTX 30 µM ($^{***}p < 0.0001$, Chi-square value = 21.59, df = 1) and to Lipo unloaded A ($^{***}p < 0.0001$, Chi-square value = 51.57, df = 1). Similar results were observed after the injection of PTX 100 µM compared to Ctrl ($^{\#\#\#}p < 0.0001$, Chi-square value = 38.10, df = 1), to LipoPTX 100 µM ($^{\#\#}p < 0.005$, Chi-square value = 8.038, df = 1), and Lipo unloaded B ($^{\#\#\#}p < 0.0001$, Chi-square value = 22.55, df = 1).

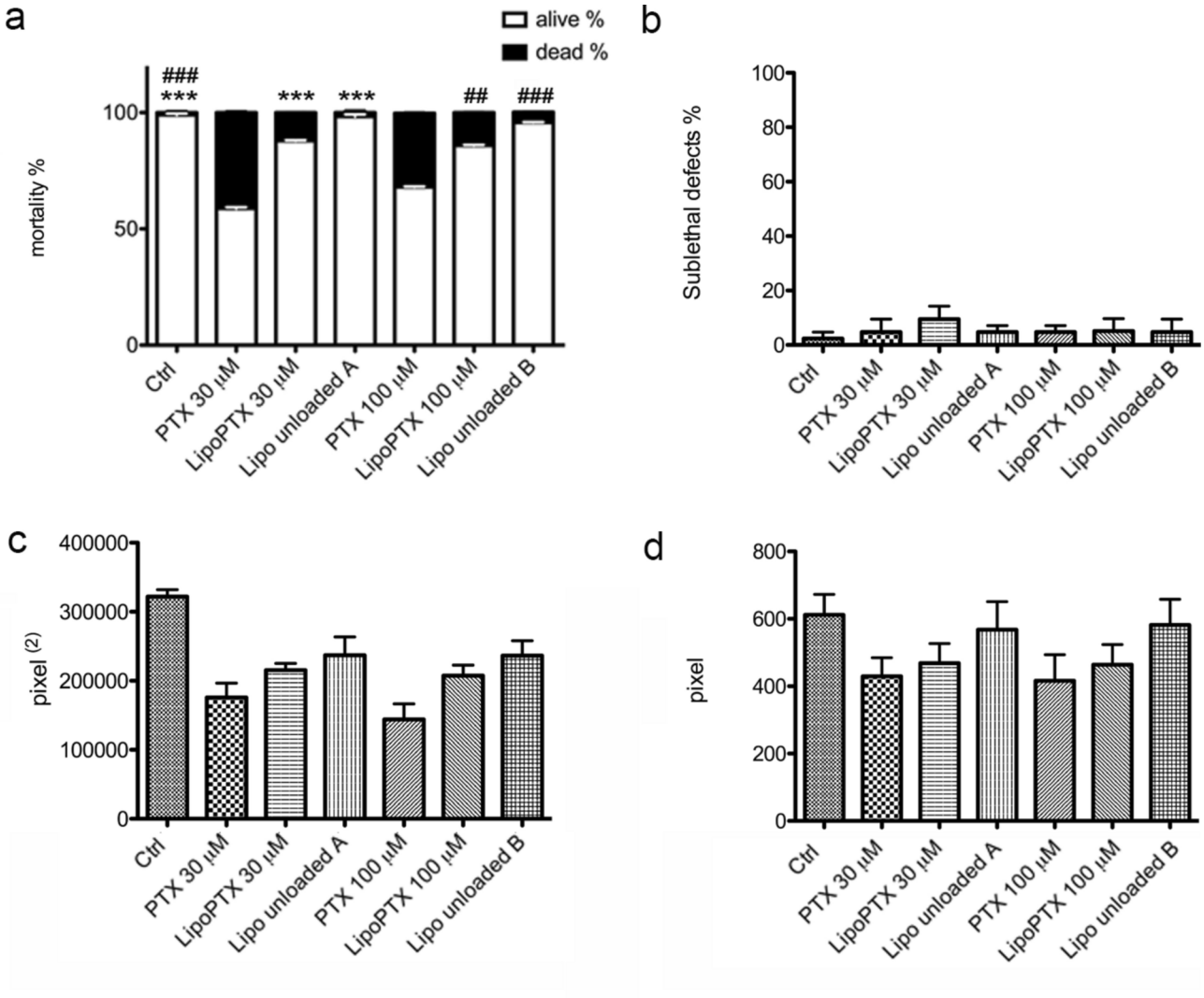

Fig. 2. Liposomes injections results. (**a**) Graph shows mortality percentages of embryos injected with liposomes loaded with PTX 30 and 100 µM, compared to embryos injected with PTX alone (30 or 100 µM) and liposomes unloaded observed during 3 independent experiments**,** for a total of n = 32 embryos for each experimental group. The liposomes unloaded are defined as A, wich are blank liposomes at liposome concentration equivalent to LipoPTX 30 µM, or B, wich are blank liposomes with liposome concentration equivalent to LipoPTX 100 µM. A high mortality percentage (40%) is observed in embryos injected with PTX 30 µM, clearly reduced in embryos injected with LipoPTX 30 µM (12%) ($^{***}p < 0.0001$). The same is observed in embryos injected with PTX 100 µM (31.6% of mortality), compared to embryos injected with LipoPTX 100 µM (14.6%) ($^{\#\#}p < 0.005$). (**b**) Graph reporting the sublethal defects observed. The most recurrent defect is cardiac edema, present in an average of 0.5% of embryos injected. (**c**, **d**) Graphs reporting analyses on GFP fluorescent signal and on peripheral sensory neurons length measures at 48 h post injection.

The sublethal defects observed (Fig. 2b) were specifically cardiac edema, present in 0.5% of embryos injected with LipoPTX 30 µM, corresponding to less than n = 3 ± 1 embryos observed during 6 different experiments. At 48 hpi, the embryos were analyzed under a fluorescence stereomicroscope (Fig. 2c and d). Based on the data obtained, which reported an interesting trend in embryos injected with PTX 30 µM, LipoPTX 30 µM, and Lipo unloaded A, we decided to focus on this concentration.

Liposomes characterization by dynamic light scattering and light field microscopy

3 µL of each liposome formulation and PTX was dropped on a cover slip and sealed with nail polish. Samples were stored at 4 °C and imaged at 40X magnification. We performed DLS analyses before testing them in Tg(*isl2b*:GFP)^{zb7} transgenic embryos and compared their effect to liposomes that were not functionalized (Table 1).

We tested the ζ-Average, polydispersion index and ζ-potential at 0, 24 and 48 h to verify if there were some changes in liposomes during time.

	L_t[a]	L_t[a]	S_t[b]	DOTAP[c]	DOPC[d]	PTX	[PTX]	[PTX]	MSLP[e]	V_f[f]
	mM	mg	Mg	mol%	mol%	mol%	ug mL^{-1}	uM	mol%	mL
Lipo	1	0.74	0.74	50	50	0	0	0	0	1
LipoPTX		0.72	0.74		47	3	25.6	30	0	
MSLP-Lipo		0.71	0.76		45.34	3	25.6	30	1.66	

Table 1. Liposomes composition a) *Lt* total lipid amount; b) *St* total solid amount; c) DOTAP was fixed at 50 mol% for all formulations; d) DOPC amount changed according to the other components amount in the formulation; e) MSPL 1.66 mol% correspond to the ratio DOTAP:MSLP (w/w) 10:1, or DOTAP:MSLP (mol/mol) 30:1; f) final formulation volume DLS analyses.

Nanoparticles	Medium	Time (h)	ζ-Average (nm) ± SD	PdI ± SD	ζ-potential ± SD (mV)
Lipo (unloaded)	mQ	0	130.7 ± 18.42	0.027 ± 0.00	39.0 ± 11.3
		24	126.2 ± 25.37	0.052 ± 0.00	41.1 ± 15.6
		48	125.4 ± 20.73	0.049 ± 0.00	40.7 ± 11.7
LipoPTX (30 µM)	mQ	0	107.9 ± 19.92	0.060 ± 0.00	44.7 ± 11.0
		24	107.0 ± 26.93	0.052 ± 0.00	46.4 ± 12.5
		48	104.2 ± 21.44	0.099 ± 0.00	42.9 ± 10.6
MSLP-Lipo (unloaded)	mQ	0	124.5 ± 14.17	0.018 ± 0.00	43.5 ± 13.9
		24	122.4 ± 19.90	0.084 ± 0.00	48.7 ± 8.55
		48	120.6 ± 30.51	0.116 ± 0.00	42.3 ± 11.7
MSLP-LipoPTX (30 µM)	mQ	0	106.2 ± 22.43	0.101 ± 0.00	45.6 ± 19.4
		24	104.0 ± 23.24	0.142 ± 0.00	49.2 ± 8.45
		48	102.7 ± 28.28	0.130 ± 0.00	41.9 ± 11.0

Table 2. DLS analyses. Size (ζ-Average (nm) and Polydispersity Index (PdI) of 30 µM Liposomes (Lipo unloaded 30 µM, LipoPTX 30 µM, MSLP-Lipo unloaded 30 µM and MSLP-LipoPTX unloaded 30 µM) measured by Dynamic Light Scattering (DLS) at different time point in mQ water. Means SD of three replicates.

The results observed showed that all the liposomes (functionalized or not and loaded with PTX or not) presented a ζ-Average of circa 131 nm as diameter, and did not exhibit relevant changes in the hydrodynamic diameter in water-based suspensions during time (Table 2). Moreover, Light field microscopy was used to observe the PTX solubility and the (Fig. 3).

Embryos injection

The embryos to be injected were mechanically chorion deprived at 24 hpf and screened for GFP signal. The 6 different experimental groups were set up as follows. (i) Ctrl; (ii) embryos injected with PTX 30 µM; (iii) embryos injected with LipoPTX 30 µM; (iv) embryos injected with Lipo unloaded; (v) embryos injected with MSLP-LipoPTX 30 µM; (vi) embryos injected with MSLP-Lipo unloaded. N = 80 embryos for each group, observed during 6 different experiments (n = 480 embryos total) were analyzed. The embryos were anesthetized and injected at 48 hpf. After the injection, the embryos were reawakened, maintained at 28 ± 1 °C and observed for defects and mortality during the following 48 h.

At 96 hpf, the embryos were analyzed, photographed under a fluorescence stereomicroscope, and successively used for the molecular analyses.

At 48 hpi, the mortality rate showed a significant increase in embryos injected with PTX 30 µM compared to Ctrl ($^{@}p = 0.0002$, two-sided), to LipoPTX 30 µM ($^{***}p = 0.0008$, two-sided), to Lipo unloaded 30 µM ($^{***}p = 0.0008$, two-sided), to MSLP-LipoPTX 30 µM ($\#p = 0{,}0192$, two-sided), and to MSLP-Lipo unloaded 30 µM ($^{***}p = 0.0008$, two-sided) (Fig. 4a). The negligible percentage of sublethal defects observed in the experimental groups, averaging 5.8%, primarily consisted of mild cardiac edemas (Fig. 4b).

Fluorescence evaluation

To deeply investigate if liposomes could reduce the possibility of incurring PTX secondary detrimental effects, such as CIPN, we examined the variations in GFP signal in transgenic Tg(*isl2b*:GFP)^{zb7} embryos injected with PTX 30 µM, LipoPTX 30 µM and MSLP-LipoPTX 30 µM compared to Ctrl not injected. The Tg(*isl2b*:GFP)^{zb7} is an advantageous zebrafish line since the RB neurons can be analyzed for axon degeneration. The differences were particularly evident in the caudal fin of zebrafish embryos at 96 hpf (Fig. 5a).

GFP signal and peripheral sensory neurons length were measured in n = 6 embryos at 96 hpf related to (i) Ctrl; (ii) embryos injected with PTX 30 µM; (iii) embryos injected with LipoPTX 30 µM, and (iv) embryos injected with MSLP-LipoPTX 30 µM, obtained during 6 different experiments, for a total of n = 36 embryos for each experimental group examined.

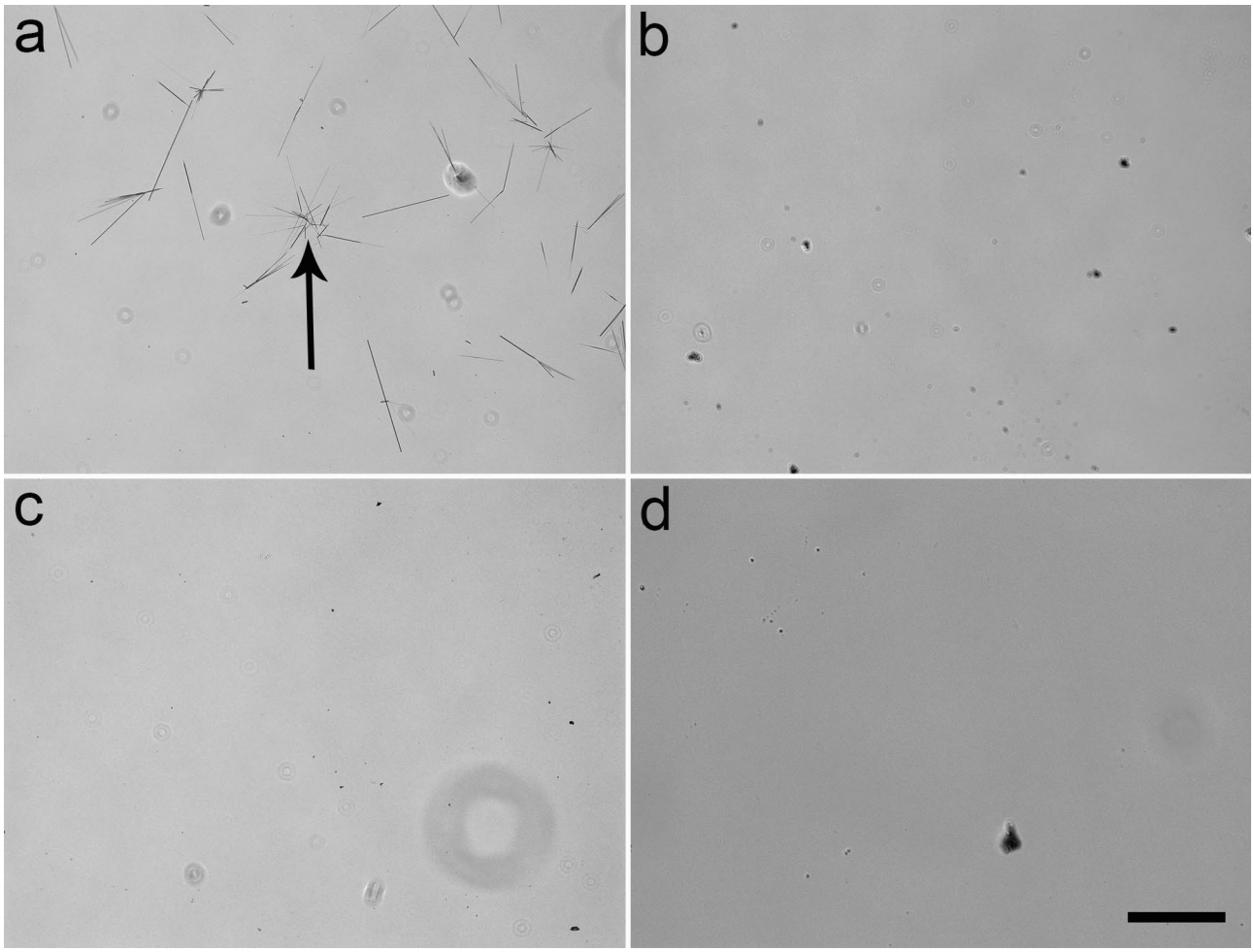

Fig. 3. Selected light field microscopy images of PTX crystals and liposome formulations. Light-field microscopy was used to observe PTX crystal formation. (**a**) PTX crystals are present in the higher concentration 0.5 mM PTX mixture in H_2O/methanol 1:1 (arrow). (**b**–**d**) Images showing liposome formulations MSLP-Lipo unloaded (**b**), LipoPTX (**c**), and the complete formulation MSLP-LipoPTX (**d**), prepared at 3 mol%. Scale bar (50 µM).

The results showed a statistically significant decrease in GFP signal area (reported in arbitrary units) in embryos injected with PTX 30 µM, compared to Ctrl embryos (Ctrl vs. PTX 30 µM, $^{**}p < 0.005$). The embryos injected with LipoPTX 30 µM and MSLP-LipoPTX 30 µM showed no statistically significant differences in GFP signal compared to PTX 30 µM injected embryos (Fig. 5b).

The measurement of peripheral sensory neurons extent showed a significant reduction in the average length in embryos injected with PTX 30 µM, compared to Ctrl embryos, while an increasing trend was observed in liposomes-injected embryos (Fig. 5c).

Behavioral test and caudal fin morphological observation

Being CIPN the cause of movement impairment, we analyzed the embryos touch-provoked mobility behavior by the Touch evoke response test, in which the number of evoked escape events was recorded for each embryo after a gentle touch. No significant differences between Ctrl embryos and embryos of each experimental group were observed, even if the trend showed a decrease in embryos that did not respond to the stimulus in LipoPTX 30 µM, Lipo unloaded, MSLP-LipoPTX 30 µM and MSLP-Lipo unloaded injected embryos compared to embryos injected with PTX 30 µM (Supplementary Fig. 2a).

The morphology of the caudal fins of embryos injected at 96 hpf was observed to verify the PTX damage in the caudal fin extremities (Fig. 5a, white arrows). Even if not statistically significant, the results showed an increase in the percentage of embryos injected with PTX 30 µM presenting caudal fin damages compared to all the other experimental groups observed (Supplementary Fig. 2b).

Molecular evaluation of PTX effects

The expression levels of *nfkb2, tnfα, il1β, il6, tgfβ1a, tgfβ1b and tgfβ3* genes, related to neuropathic pain caused by PTX were investigated by qRT-PCR (Fig. 6). The RNAs of embryos injected with PTX 30 µM, LipoPTX 30 µM

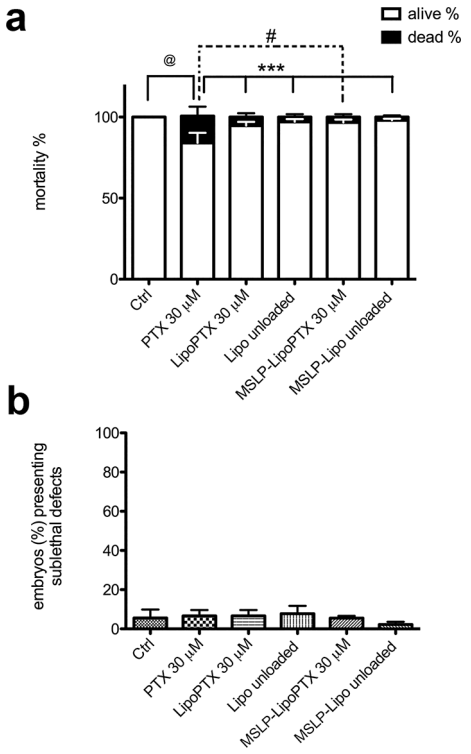

Fig. 4. Paclitaxel and liposomes injections results in embryos at 48 hpi (**a**) Graph reporting the mortality average percentage of embryo injected with PTX 30 µM, compared to Ctrl and LipoPTX 30 µM, Lipo unloaded, MSLP-LipoPTX 30 µM and MSLP-Lipo unloaded injected embryos. The number of embryos observed was n = 13 embryos for each group ($n_{total} = 80$), in 6 different experiments. At 48 hpi, the mortality rate showed a significant increase in embryos injected with PTX 30 µM compared to Ctrl ($^{@}p = 0.0002$, two-sided), to LipoPTX 30 µM ($^{***}p = 0.0008$, two-sided), to Lipo unloaded 30 µM ($^{***}p = 0.0008$, two-sided), to MSLP-LipoPTX 30 µM ($^{\#}p = 0.0192$, two-sided), and to MSLP-Lipo unloaded 30 µM ($^{***}p = 0.0008$, two-sided). For statistical analyses, the Fisher's exact test was applied. (**b**) Graph reporting the negligible percentage of sublethal defects observed (cardiac edemas), also detected in Ctrl not injected. The results showed that either functionalized or not liposomes were well tolerated by the embryos, and their stability in the biological milieu allowed protection against the PTX action in the healthy tissues for the 48-h period observed.

or MSLP-LipoPTX 30 µM were compared to Ctrl embryos RNAs. The RNAs were extracted and processed from embryos at 96 hpf of 6 different experiments.

The results showed that in most cases, these genes were upregulated in embryos injected with PTX 30 µM, compared to Ctrl embryos and both liposomes injected embryos, except for *tgfβ1b* expression level, for which a downregulation was observed. A statistically significant downregulation of *nfkb2* in embryos injected with LipoPTX 30 µM was observed, compared to embryos injected with PTX 30 µM, while in embryos injected with MSLP-Lipo PTX 30 µM, only a downregulated trend was observed.

The results observed after the analyses of *bax, bcl2, Mn-sod, Cu/Zn-sod*, *catalase* and *glutathione peroxidase,* a panel of genes related to reactive oxygen species (ROS), showed a decreased trend in the gene expression levels observed in embryos injected with liposomes loaded with PTX 30 µM compared to embryos injected with PTX 30 µM.

Discussion

Zebrafish is an attractive in vivo model for evaluating nanocarrier performance and toxicity studies. Along with its numerous characteristics, such as the high fecundity, transparency of the embryos, and simplicity of structures, it supports the obtention of significant results related to the design and development of new therapeutic strategies.

In our study, Tg(*isl2b:*GFP)^{zb7} transgenic embryos were used, a zebrafish line particularly convenient in studying CIPN, one of the most detrimental side effects of PTX in patients experimenting with cancer. In our strategy, the final purpose was to take advantage of zebrafish embryos to assess the in vivo effects of PTX , evaluate toxicity and CIPN at molecular, behavioral and microscopy levels, and propose the development of a therapeutic system such as liposomes, which are effective to reduce the PTX outcomes and stable enough to resist in a biological milieu.

Firstly, we decided on the preferable injection site, at what developmental stage to inject, and which PTX concentration to use. The need to test different concentrations of drugs is related to the fact that, in zebrafish embryos, there is a lack of standardized protocols for pharmacological dose administration, such as those

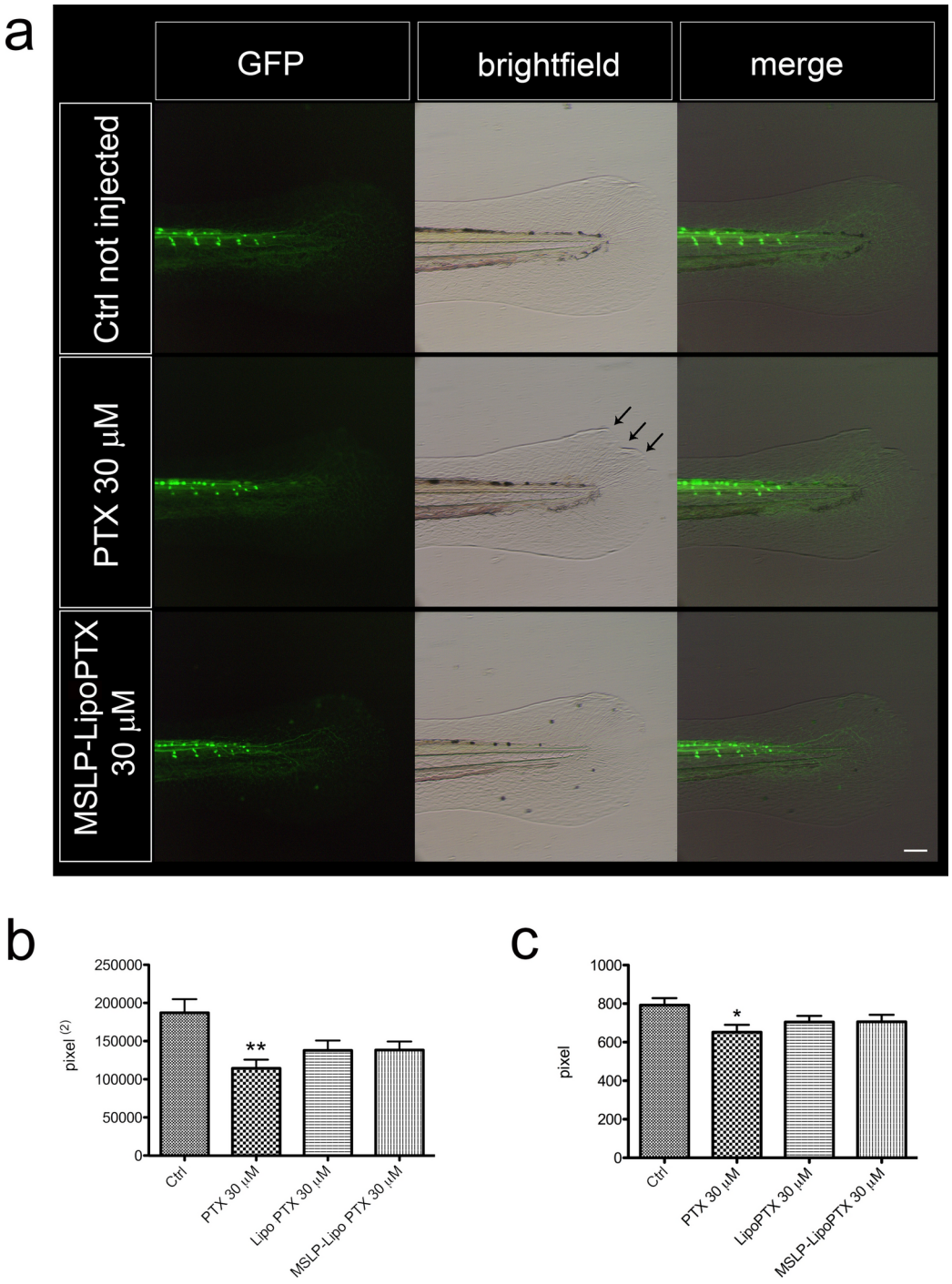

Fig. 5. Variations in GFP expression in Tg(*isl2b*:GFP)^{zb7} injected embryos. (**a**) Representative images of injected embryos at 96 hpf. The images show the caudal fin morphology. In PTX 30 µM injected embryos, there are evident defects affecting the fin extremity related to PTX action (black arrows). Since the embryos injected with LipoPTX 30 µM and MSLP-LipoPTX 30 µM showed very similar results, only MSLP-LipoPTX 30 µM embryos image were reported as an example (Scale bar, 50 µm). (**b**) The graph reports a statistically significant decrease in GFP signal area (reported in arbitrary units) in embryos injected with PTX 30 µM, compared to Ctrl embryos (**$p < 0.005$). The embryos injected with LipoPTX 30 µM and MSLP-LipoPTX 30 µM showed no statistically significant differences in GFP signal compared to PTX 30 µM injected embryos. Nonetheless, an increasing trend in the GFP signal is visible. (**c**) Graph showing results of peripheral sensory neurons extent measures. The length is taken from the fourth from the last RB neuron to the extremity of the caudal fin. In this case, a significant reduction was observed in the average length of peripheral sensory neurons in embryos injected with PTX 30 µM, compared to Ctrl embryos, while an increasing trend was observed in liposomes-injected embryos.

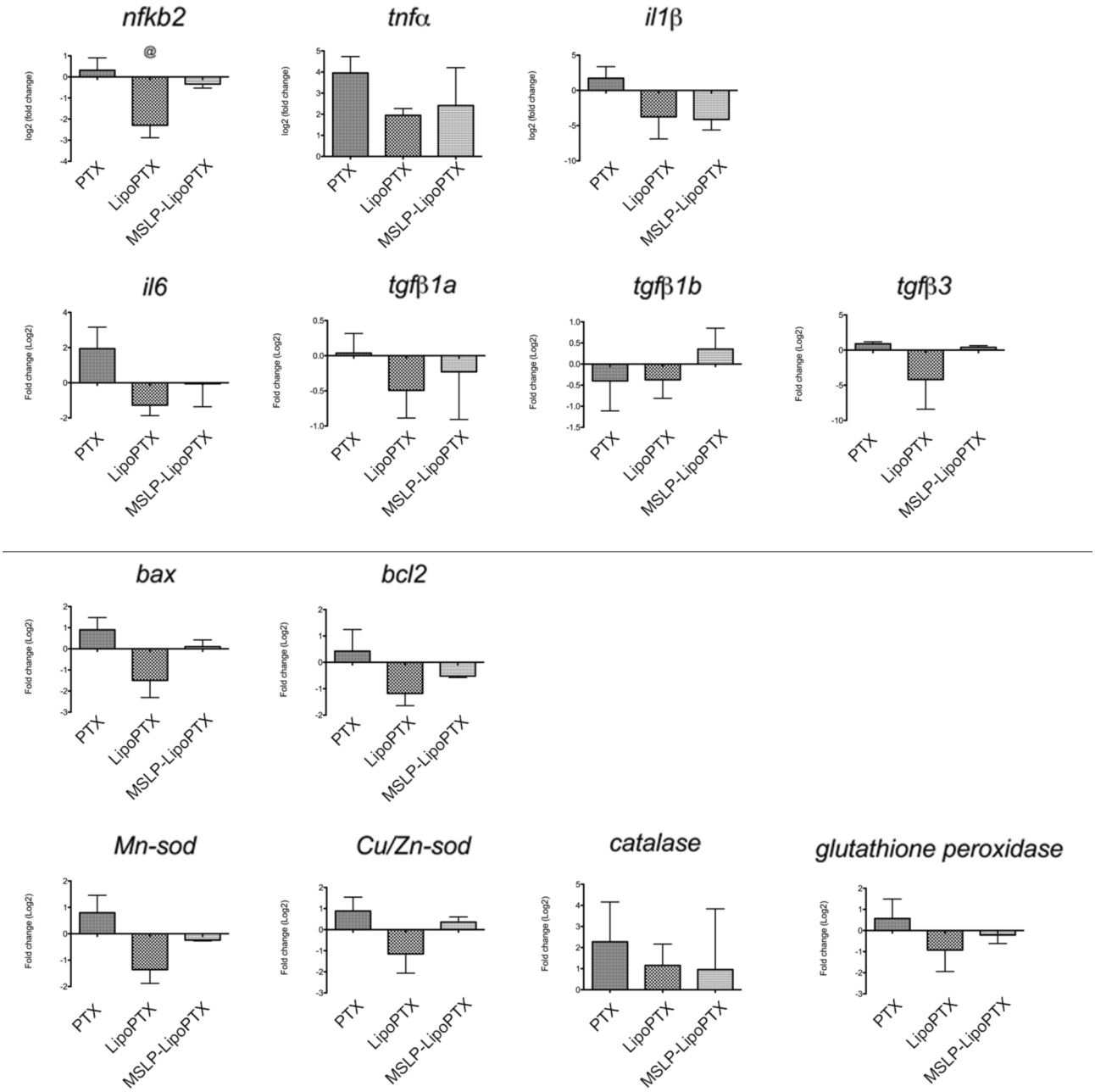

Fig. 6. Molecular investigations of liposomes effects compared to PTX. (**Upper panel**) Graphs reporting gene expression levels of *nfkb2, tnfα, il1β, il6, tgfβ1a, tgfβ1b* and *tgfβ3*, a panel of genes reported in literature as related to CIPN. The results showed that the genes related to neuropathic pain are generally upregulated in embryos injected with PTX 30 µM, compared to Ctrl embryos and both liposomes injected embryos. *nfkb2*, a key regulator of molecul es and pathways important for inflammation and pain, is significantly downregulated ($^{@}p = 0.022$) by LipoPTX 30 µM injection. (**Lower panel**) Graphs show expression levels of genes related to oxidative stress. The presence of increased ROS is known to be caused by the PTX exposure. Our results showed a decreasing trend in all the gene expression levels observed after injection with liposomes.

available for higher mammals[22]. This is due to the presence of many administration routes for therapeutical agents in such a model, namely injection or epidermal contact, and to the impossibility of weighing each embryo prior the treatment as in other animals[23]. Nonetheless, the advantages of this model, such as the ability to test multiple concentrations simultaneously, rapid development, the possibility to assess drug outcomes at various stages, and ease of manipulation, far outweigh the challenges.

The timeframe and the site of injection chosen for *Tg(isl2b:GFP)*^{zb7} embryos were based on the fact that the final purpose will be testing the efficacy in reaching the target of functionalized liposomes in a xenograft model generated using human breast cancer cells. There are many paths used to set up a xenograft model in zebrafish embryos, such as the yolk sac, the duct of Cuvier, also known as the common cardinal vein, the caudal

vein, perivitelline space, and hindbrain ventricle[24,25]. To be minimally invasive as possible after the xenograft transplantation in further studies, we have established the injection of PTX and liposomes using a volume of 1 nanoliter (nL) directly into the yolk sac, close to the sub-intestinal vein (SIV) plexus. A xenograft model in embryos at 24 hpf will be generated, and the larvae will be injected with drugs the following day, at 24 h post-injection (hpi), letting the tumoral cells grow for 24 h. For this reason, the injection of PTX and liposomes in embryos at 48 hpf was selected.

We then assessed different PTX concentrations to observe and identify defects associated with drug administration, thereby determining the proper amount of PTX to be incorporated in the liposomes. In the literature, numerous scientific papers report concentrations of PTX used in both in vitro[26,27] and in vivo models[28–30]. Considering the research work of Lisse and colleagues[31], who injected PTX in zebrafish embryos at a concentration of 22 μM, we decided to inject at 48 hpf the Tg(*isl2b*:GFP)^{zb7} embryos at a concentration of 60 nM, 100 nM, 10 μM and 22 μM PTX in 1 nL. The results showed a mortality rate of less than 5% and a sublethal defect rate lower than 1%. Furthermore, as a readout of CIPN, we analyzed the fluorescence signal of caudal fin embryos at 48 h post-injection (hpi). Also, in this case, no significant results were observed. Therefore, a decision was taken to produce liposomes loaded with higher PTX concentrations, such as 30 μM and 100 μM. Both concentrations exceeded the highest PTX concentration tested so far, but this was necessary to observe differences after the injections of PTX-loaded liposomes..

After PTX 30 μM injection, a mortality rate of 40% was obtained, clearly reduced in embryos injected with LipoPTX 30 μM (12%). The same was observed in embryos injected with PTX 100 μM (31.6% of mortality), compared to embryos injected with LipoPTX 100 μM (14.6%).

Moreover, the injection of 30 μM PTX, LipoPTX and Lipo unloaded showed a negligible number of embryos presenting sublethal defects.

Since there was evidence in the literature that even low doses of PTX are effective in the tumor environment[39], we hypothesized that PTX 30 μM was a suitable dosage compromise to observe defects and differences in the easier way comparing embryos injected with liposomes loaded with the same PTX amount. Furthermore, we were confident in increasing the quantity of PTX injected in embryos concerning the dose of 22 μM that Lisse and colleagues used[36] because, with a different approach, we focused on performing a unique injection, considering the generation of a xenograft model for our upcoming studies. We decided to focus on this concentration (30 μM) for these reasons.

Liposomes functionalized with an MMP-sensitive lipopeptide for an MMP-triggered PTX (MPLS-LipoPTX) were prepared for the PTX release in the tumor site and evaluation of the behavior of the nanostructure in vivo, comparing them to PTX (solution) and Liposomes without functionalization.

Before injection, the liposomes were characterized by Light field microscopy and DLS. The DLS results showed a PDI way lower than ≤ 0.3 (in a range from 0.018 to 0.142), underlining that all the liposome formulations were monodispersed. The stability was also confirmed by the ζ-potential values observed, which were over 30 mV for each specimen. It is known that a high ζ-potential is related to stability since the charged particles repel one another, overcoming the tendency to form aggregates[32,33].

Microscopy was used to observe PTX crystal formation. Figure 3 a presents the PTX crystals from a 0.5 mM PTX mixture in H2O.methanol 1:1, a high concentration in which crystals are observed. Figure 3b, c, and d represent liposome formulations MSLP-Lipo unloaded, LipoPTX, and the complete formulation MSLP-LipoPTX, respectively, prepared at 3 mol%, a fraction presented in all animal studies and clinical trials with liposomes. In our studies, the amount of PTX was not higher than the liposomes membrane solubility, and PTX remains soluble in the lipid bilayer and is has not phase separated into stable water-insoluble crystals.

Liposome stability is fundamental for this therapeutic system's final purpose. Sure enough, liposomes must reach the target entirely before their disruption and releasing their cargo, thus leading to a specific drug action exclusively in the target site and consequently to a reduction of the side effects of the treatment, potentially increased by the no-needed activity exerted in healthy districts. However, further investigations are needed to explore the impact of the lipopeptide on liposome stability after 72 h of film hydration.

The results observed at 48 hpi showed that mortality of embryos injected with LipoPTX 30 μM, Lipo unloaded, MSLP-LipoPTX 30 μM, and MSLP-Lipo unloaded was significantly reduced compared to PTX 30 μM injected embryos and resulted like mortality observed in Ctrl embryos at the same developmental stage. Moreover, the embryos presenting sublethal defects were a negligible number within the experimental groups observed. Since these were observed also in Ctrl not injected, we were confident that they were not triggered by the injection or the injected material.

The results obtained underlined the stability of the two different liposomes injected, functionalized or not, during the 48 h of observation, besides the effective reduction of free PTX injection effects, emphasizing the proper role that this therapeutic strategy has, and the fact that the different liposomes were well tolerated by the embryos (mortality rate averaged 3.4%, with sublethal defects averaging 5.8%, and no significant upregulation or downregulation of gene expression levels was observed).

The injection and evaluation of unloaded liposomes were important to understand if the synthesized liposomes, the MMP-sensitive lipopeptide used as functionalization, or the injections themselves can be toxic or cause the defects observed. Their role is to be a positive control for the experiments with embryos and the chemical synthesis.

At this point, to evaluate if liposomes were reducing the effects of PTX on CIPN, we assessed the fluorescent analyses on transgenic embryos injected. In this case, the embryos injected with LipoPTX 30 μM and MSLP-LipoPTX 30 μM showed no statistically significant differences in GFP signal compared to PTX 30 μM injected embryos. Nevertheless, a trend of increasing GFP signal was observed.

No significant differences were observed also in peripheral sensory neurons extent after injection of liposomes and free PTX. In this case, the length of peripheral sensory neurons departing from the fourth from the last RB neuron[34] to the extremity of the caudal fin.

Since PTX-induced epithelial damage precedes cutaneous axon degeneration, as reported by Lisse and colleagues[31], and probable movement impairment, we observed the behavior of embryos after the stimulus and the morphology of caudal fins of embryos injected at 96 hpf.

About the behavioral evaluation, no significant differences between Ctrl embryos and embryos of each experimental group after the touch evoked test were observed, even if the trend showed an increase in embryos number that responded to the stimulus in LipoPTX 30 μM, Lipo unloaded, MSLP-LipoPTX 30 μM and MSLP-Lipo unloaded injected embryos compared to embryos injected with PTX 30 μM.

About the morphology, the evaluation of injuries in caudal fin extremities presented some issues since defects in caudal fins were present even in Ctrl embryos, probably ascribable to the manipulation of embryos. Additionally, in this case, the percentage of embryos injected with PTX 30 μM increased compared to embryos injected with liposomes and Ctrl, although this was not statistically significant.

Our general thought is that we obtained no statistically significant results in both behavioral test and morphological evaluation since the time elapsed between the PTX injection and observation was insufficient to appreciate severe damage. Nonetheless, the interesting decreasing trend in embryos injected with liposomes, compared to embryos injected with PTX, led us to hypothesize that these nanocarriers can effectively reduce the defects caused by the PTX anti-cancer drug in terms of behavior and morphology of embryos.

Future experiments with an extended timeframe or repeated liposome injections will be necessary and valuable to provide clearer evidence of the non-harmful effects of liposomes on behavior and morphology.

Finally, we evaluated the PTX 30 μM effects at molecular level, comparing the results obtained with the different liposomes injection.

We decided to analyze a panel of genes based on the results reported by North et al.[35]. North and colleagues tried correlating the neuropathic pain caused by PTX and differentially expressed genes at the transcriptomic level. In this regard, we investigated the expression level of *nfkb2, tnfα, il1β, il6, tgfβ1a, tgfβ1b and tgfβ3* by qRT-PCR.

To perform the analyses, the RNAs of embryos injected with PTX 30 μM, LipoPTX 30 μM or MSLP-LipoPTX 30 μM were compared to Ctrl embryos RNAs.

The results obtained showed an upregulation of most of the genes analyzed in embryos injected with PTX 30 μM, compared to Ctrl embryos and both liposomes injected embryos, except for *tgfβ1b* expression level, for which a downregulation was observed. The only gene expression level that showed a statistical downregulation in embryos injected with non-functionalized liposomes is *nfkb2*. This gene encodes a subunit of the transcription factor complex nuclear factor-kappa-B (*NFkB*), a key regulator of molecules and pathways important for inflammation and pain[36].

The statistically significant downregulation was observed specifically in embryos injected with LipoPTX 30 μM, compared to embryos injected with PTX 30 μM, while in embryos injected with MSLP-Lipo PTX 30 μM, only a downregulated trend was observed.

Furthermore, we observed a panel of genes, such as *bax, bcl2, Mn-sod, Cu/Zn-sod*, *catalase* and *glutathione peroxidase*, to evaluate the role of reactive oxygen species (ROS) in the development and maintenance of PTX-induced painful neuropathy[37].

The results showed a decreased trend in the gene expression levels observed in embryos injected with liposomes loaded with PTX 30 μM compared to embryos injected with PTX 30 μM, thus underlining the positive effect of both liposomes in reducing oxidative stress impairment compared to free PTX. We hypothesize that the not statistically significant results are due to the reduced treatment timeframe, which was only 48 h. Altogether, the encouraging results obtained in our research confirmed the positive effect of liposomes, functionalized or not, in reducing PTX side effects, such as CIPN at molecular, behavioral and microscopy levels. Furthermore, led us to hypothesize that the liposomes may demonstrate in vivo stability.

To conclude, this study presented the zebrafish embryos not only as an in vivo valuable model for testing novel therapeutic strategies but also as a model that helps the step-by-step production of new therapeutic approaches. The embryos offer invaluable benefits by allowing researchers to investigate effects at multiple levels while simultaneously evaluating the mechanisms involved and activated during treatment.

The opportunity to assess directly and in vivo the toxicological profile of a novel drug nanocarrier strategy is invaluable and requires appropriate models, as we demonstrated that the zebrafish embryos are. They can be considered a bridge model between in vivo and in vitro models, giving the chance to evaluate an integrated response that considers development progression and systemic diffusion, for example. Moreover, further research on the promising liposome nanocarrier system would not be wasted and is indispensable for newer insights that can lead to possible breakthroughs in fighting CIPN.

Materials and methods

Animal rearing and ethics

The adults of the *Tg(isl2b:GFP)*^{zb7} transgenic line (Tu/Longfin background) were kindly donated by the Max-Planck Institute for Biological Intelligence (Am Klopferspitz 18, 82,152 Martinsried Germany), maintained and bred at the University of Milano-Bicocca Zebrafish Facility (approved by ATS Metro Milano Prot. n. 0020984—12 February 2018), in a recirculating ZebTec Active Blue aquatic system (Tecniplast, Buguggiate, Italy). All experiments were performed on embryos within 5 days post fertilization (dpf), thus not subject to animal experimentation rules according to European and Italian directives. Embryos were raised at 28 °C and staged according to Kimmel et al.[38]. The embryonic ages were expressed in hours post fertilization (hpf) and days post fertilization (dpf).

Liposome preparation and chemicals

Liposomes containing PTX (LC Laboratories, Woburn, MA) (LipoPTX) and liposomes containing PTX and metallosensitive lipopeptide (MSLP) (MSLP-LipoPTX) were prepared after choosing the main components of the nanoformulation. DOTAP (SC-208,732, Santa Cruz Biotechnology, USA), a cationic phospholipid, was selected as the fixed amount component in the formulation (50 mol% of the total phospholipid amount. DOPC amount corresponds to 50 mol% in the unloaded liposomes and 47 mol% in the LipoPTX, as PTX in such formulation corresponds to 3 mol%. Previous studies have also reported DOTAP and DOPC as the main phospholipid components for the PTX incorporation and release[39,40]. Formulations were prepared by film formation and hydration followed by extrusion in a thermobarrel. The PTX amount in the formulation was selected due to the previous studies about the PTX instability when the drug's incorporation in the liposome bilayer is higher than 3 mol% (Table 1).

Light field microscopy was used to observe the PTX solubility. Samples were prepared and assayed after 72 h. 3 µL of each liposome formulation and PTX was dropped on a cover slip and sealed with nail polish. Samples were stored at 4 °C and imaged at 40X magnification.

PTX and liposome nanoformulation injection

The embryos were injected at 48 hpf in the upper site of the yolk, close to the SIV, with a volume of 1 nl. Briefly, the embryos at 24 h were mechanically chorion deprived, screened for fluorescence signal and then maintained in grow medium at 28.5 °C. Shortly before the injection, the embryos were anesthetized with 0.016% ethyl 3-aminobenzoate methanesulfonate salt (Tricaine, Sigma Aldrich, Saint Louis, MO). Before the injection, the PTX (LC Labs, Boston, USA) was suspended using sterile DMSO 200 mg/ml (Sigma-Aldrich, Saint Louis, MO) to obtain a stock solution of 50 mM (mM). To reach the injection concentration, we diluted the stock solution with milliQ water each time before injection. This resulted in a DMSO percentage lower than 1%, the maximum percentage tolerated in zebrafish embryos.

PTX or liposome nanoformulation injection was made in embryos at 48 hpf using a microinjection station (FemtoJet 4i, Eppendorf, Hamburg, Germany). The solvent used for both was milliQ water plus phenol red as vital tracker. The injected embryos were then rescued in a growth medium solution, to which 0.003% 1-phenyl-2-thiourea (PTU, Sigma-Aldrich, Saint Louis, MO) was added to prevent pigmentation. At 96 hpf, embryos were placed in a 60 mm Petri dish with a medium containing Tricaine, and a single-plane image was acquired using a Leica M205FA microscope equipped with a 5MPx DFC450C digital camera and Leica software (Leica, Leica Application Suite X, version 3.7.0.20979, https://www.leica-microsystems.com/products/microscope-software/p/leica-las-x-ls/), and successively used for molecular analyses.

The injection at 48 hpf developmental stage is based on several factors. First, the human breast cancer cell xenograft model will be established at 24 hpf. Second, vascular development plays a crucial role, as primary blood vessels form within the first 24 h, followed by the sprouting angiogenesis of intersegmental blood vessels (ISVs). By 48 hpf, blood circulates anteriorly and posteriorly through a series of aortic arteries forming a circulatory loop. The ISVs in the trunk and tail become fully functional after 72 hpf[41]. Therefore, we hypothesized that the optimal timeframe for observing liposome effects is between 48 and 96 hpf.

Characterization of liposomes

Physicochemical properties of LipoPTX and MSLP-LipoPTX, such as hydrodynamic size (D_h), polydispersity (PDI), and charge (z-pot), were determined during the set-up of the formulation. For that, dynamic light scattering (DLS) using Zetasizer® Nano-ZS90 (Malvern Instruments, Malvern, UK). DTS0012 cuvettes were used to measure the D_h and the PDI, whereas, for the determination of the z-pot, DTS1070 cuvettes were selected. All determinations were performed in the raw sample (dilution in MilliQ water 1:2) in triplicate at 25 °C. The maximum acceptable value for the sample monodisperse was a PDI ≤ 0.3.

The Light field microscope (Widefield Microscopes Zeisscell observer, Zeiss, Oberkochen, Germany) was used for morphological characterization of liposomes and PTX solubility evaluation at the microscopy level.

RNA extraction and cDNA synthesis

Total RNA was extracted, as reported in Bragato et al.[42]. Briefly, total RNA derived from zebrafish embryos at 96 hpf was processed using TRI Reagent (MRC, Cincinnati, OH, USA). First-strand cDNA synthesis reaction from total RNA was catalyzed by High-Capacity cDNA Reverse Transcription Kit (ThermoFisher Scientific, Applied Biosystems).

The cDNA was then amplified with Actin-β primers (Fw: 5′-TGTTTTCCCCTCCATTGTTGG-3′, Rw: 5′-TTCTCCTTGATGTCACGGAC-3′) using Phusion High-Fidelity polymerase (Finnzymes, Thermo Fisher Scientific, Waltham, MA, USA).

Real-time quantitative PCR

Quantitative real-time PCR (qRT-PCR) was performed as reported in Bragato et al.[43]. Briefly, the PowerTrack™ SYBR™ Green Master Mix kit (Applied Biosystems, Waltham, MA, USA) and the Quantum 3™ (Applied Biosystems, Waltham, MA, USA) Real-Time PCR system was used according to manufacturer instructions. Real-time PCR was performed in a 10 µL reaction containing 600 nM of each primer, 2 µL template cDNA, and 5 µL qPCR Master Mix. The PCR was run at 95 °C for 60 s, followed by 40 cycles of 95 °C for 15 s and 60 °C for 30 s. *mobk13* was used as the endogenous control.

Relative changes in gene expression between control and treated samples were determined using the $2^{-\Delta\Delta Ct}$ method[44], and the results were presented in logarithmic scale fold change[45]. The primer sequences of tested genes (*nfkb2, tnfα, il1β, il6, tgfβ1a, tgfβ1b, tgfβ3*, related to CIPN evaluation, *bax, bcl2, Mn-sod, Cu/Zn-sod, catalase,* and *glutathione peroxidase,* related to oxidative stress) are listed in Table S1.

Caudal fin fluorescence and peripheral sensory neurons length evaluation

To quantify the GFP fluorescent signal into the caudal fin and to measure the peripheral sensory neurons length, embryos were observed under a fluorescence stereomicroscope, and pictures of the entire tail, starting from the caudal prolongation area of the yolk, were collected. The green signal area (expressed as arbitrary units) was calculated by ImageJ Fiji software (https://imagej.net/Fiji) on fluorescent images taken under the same conditions, such as light exposition and frame size. Using the software, a threshold and a ROI were applied to the pictures to obtain regions of positive GFP in white and negative in black[46,47].

The same micrographs were used to measure and compare peripheral sensory neurons length in the observed experimental groups, taking advantage of the SNT-Simple Neurite Tracer plugin[48].

The GFP signal and the neuronal length measurements of injected embryos were compared to control embryos for normalization.

Behavioral test

At 48 hpi both injected and Ctrl embryos were subjected to a tactile stimulus test. A gentle stimulus was applied at the tail of the larvae using a microneedle and elicited reactions observed under a stereomicroscope. Embryos were touched, and the number of evoked escape events was recorded.

Statistical analyses

Data are reported as means and standard error of the means (SEM) using GraphPad Prism 9.2.0.332 (GraphPad Software). The statistical significance between multiple groups was determined by one-way ANOVA, followed by Bonferroni's post hoc test analysis were appropriate. The level of significance was considered at $p < 0.05$. Differences in mortality rate were assessed by the Chi-square test or Fisher's exact test, where appropriate.

Data availability

The datasets generated during the current study are available from the corresponding author upon reasonable request.

Received: 20 December 2024; Accepted: 28 April 2025
Published online: 26 May 2025

References

1. Cole, L. K. & Ross, L. S. Apoptosis in the developing zebrafish embryo. *Dev. Biol.* **240**(1), 123–142. https://doi.org/10.1006/dbio.2001.0432 (2001).
2. Reyes, R., Haendel, M., Grant, D., Melancon, E. & Eisen, J. S. Slow Degeneration of Zebrafish Rohon-Beard Neurons during Programmed Cell Death. *Dev. Dyn.* **229**(1), 30–41. https://doi.org/10.1002/dvdy.10488 (2004).
3. Liu, K. E. & Kucenas, S. Rohon-beard neurons do not succumb to programmed cell death during zebrafish development. *Dev. Biol.* **515**, 186–198. https://doi.org/10.1016/j.ydbio.2024.06.020 (2024).
4. Norton, W. H. J., Rohr, K. B. & Burnstock, G. Embryonic expression of a P2X(3) receptor encoding gene in zebrafish. *Mech. Dev.* **99**(1–2), 149–152. https://doi.org/10.1016/s0925-4773(00)00472-x (2000).
5. Palanca, A. M. S. et al. New transgenic reporters identify somatosensory neuron subtypes in larval zebrafish. *Dev. Neurobiol.* **73**(2), 152–167. https://doi.org/10.1002/dneu.22049 (2013).
6. Maklad, A. et al. The EGFR is required for proper innervation to the skin. *J. Investig. Dermatol.* **129**(3), 690–698. https://doi.org/10.1038/jid.2008.281 (2009).
7. Sagasti, A., Guido, M. R., Raible, D. W. & Schier, A. F. Repulsive interactions shape the morphologies and functional arrangement of zebrafish peripheral sensory arbors. *Curr. Biol.* **15**(9), 804–814. https://doi.org/10.1016/j.cub.2005.03.048 (2005).
8. McGraw, H. F., Nechiporuk, A. & Raible, D. W. Zebrafish dorsal root ganglia neural precursor cells adopt a glial fate in the absence of neurogenin1. *J. Neurosci.* **28**(47), 12558–12569. https://doi.org/10.1523/JNEUROSCI.2079-08.2008 (2008).
9. Cirrincione, A. M. & Rieger, S. Analyzing chemotherapy-induced peripheral neuropathy in vivo using non-mammalian animal models. *Exp. Neurol.* **323**(August), 113090. https://doi.org/10.1016/j.expneurol.2019.113090 (2020).
10. Li, R. J. et al. All-trans retinoic acid stealth liposomes prevent the relapse of breast cancer arising from the cancer stem cells. *J. Control. Release* **149**(3), 281–291. https://doi.org/10.1016/j.jconrel.2010.10.019 (2011).
11. Grace, V. M. B., Wilson, D. D., Guruvayoorappan, C., Danisha, J. P. & Bonati, L. Liposome nano-formulation with cationic polar lipid DOTAP and cholesterol as a suitable pH-responsive carrier for molecular therapeutic drug (all-trans retinoic acid) delivery to lung cancer cells. *IET Nanobiotechnol.* **15**(4), 380–390. https://doi.org/10.1049/nbt2.12028 (2021).
12. Elshennawy, A. Navigating the intricacies of breast cancer histological terrain and the efficacy of paclitaxel as a chemotherapeutic arsenal. *Octahedron Drug Res.* https://doi.org/10.21608/odr.2024.267267.1036 (2024).
13. Lastair, A., Ood, J. J. W., Owinsky, R. K. R., Oss, R., Onehower, C. D. *Drug Therapy*, (1995).
14. Schiff, D., Wen, P. Y., van den Bent. M. J. *Neurological adverse effects caused by cytotoxic and targeted therapies*, https://doi.org/10.1038/nrclinonc.2009.128 (2009).
15. Haddad, R., Alrabadi, N., Altaani, B. & Li, T. Paclitaxel drug delivery systems: Focus on nanocrystals' surface modifications. *Polymers (Basel)* **14**(4), 658. https://doi.org/10.3390/polym14040658 (2022).
16. Zajaczkowską, R., Kocot-Kępska, M., Leppert, W., Wrzosek, A., Mika, J., Wordliczek, J. *Mechanisms of chemotherapy-induced peripheral neuropathy* Mar. 02, *MDPI AG*. https://doi.org/10.3390/ijms20061451 (2019).
17. Avallone, A., Bimonte, S., Cardone, C., Cascella, M. & Cuomo, A. Pathophysiology and therapeutic perspectives for chemotherapy-induced peripheral neuropathy. *Int. Instit. Antican. Res.* https://doi.org/10.21873/anticanres.15971 (2022).
18. Wang, H., Wan, X., Wang, X., Li, M. & Tang, D. Ultrathin mesoporous BiOCl nanosheets-mediated liposomes for photoelectrochemical immunoassay with in-situ signal amplification. *Biosens. Bioelectron.* https://doi.org/10.1016/j.bios.2023.115628 (2023).
19. Giofrè, S. et al. Dual functionalized liposomes for selective delivery of poorly soluble drugs to inflamed brain regions. *Pharmaceutics* https://doi.org/10.3390/pharmaceutics14112402 (2022).
20. Goździalska, A. et al. Expression of metalloproteinases (MMP-2 and MMP-9) in basal-cell carcinoma. *Mol. Biol. Rep.* **43**(10), 1027–1033. https://doi.org/10.1007/s11033-016-4040-9 (2016).
21. Fouad, H., Salem, H., Ellakwa, D. E. S. & Abdel-Hamid, M. MMP-2 and MMP-9 as prognostic markers for the early detection of urinary bladder cancer. *J. Biochem. Mol. Toxicol.* https://doi.org/10.1002/jbt.22275 (2019).

22. Theiner, T. et al. Novel protocol for multiple-dose oral administration of the L-type Ca^{2+} channel blocker isradipine in mice: A dose-finding pharmacokinetic study. *Channels* https://doi.org/10.1080/19336950.2024.2335469 (2024).
23. Oghenesuvwe Earnest, E. Lotanna Ajaghaku, D. *Guidelines on dosage calculation and stock solution preparation in experimental animals' studies*, 2014. [Online]. Available: https://www.researchgate.net/publication/287995503
24. Veinotte, C. J., Dellaire, G. & Berman, J. N. *Hooking the big one: The potential of zebrafish xenotransplantation to reform cancer drug screening in the genomic era* (Company of Biologists Ltd, 2014). https://doi.org/10.1242/dmm.015784.
25. Lenard, A. et al. Endothelial cell self-fusion during vascular pruning. *PLoS Biol.* https://doi.org/10.1371/journal.pbio.1002126 (2015).
26. N. M. Patel *et al.*, "Paclitaxel sensitivity of breast cancer cells with constitutively active NF-kB is enhanced by IkBa super-repressor and parthenolide." [Online]. Available: www.nature.com/onc
27. Montero, P. et al. Paclitaxel-induced epidermal alterations: An in vitro preclinical assessment in primary keratinocytes and in a 3D epidermis model. *Int. J. Mol. Sci.* https://doi.org/10.3390/ijms23031142 (2022).
28. Pedro, I. D. R. et al. Optimization and in vitro/in vivo performance of paclitaxel-loaded nanostructured lipid carriers for breast cancer treatment. *J. Drug Deliv. Sci. Technol.* https://doi.org/10.1016/j.jddst.2019.1013703 (2019).
29. Cavaletti, G. et al. Translation of paclitaxel-induced peripheral neurotoxicity from mice to patients: The importance of model selection. *Pain* https://doi.org/10.1097/j.pain.0000000000003268 (2024).
30. Liu, X. et al. Paclitaxel induces neurotoxicity by disrupting tricarboxylic acid cycle metabolic balance in the mouse hippocampus. *J. Toxicol.* https://doi.org/10.1155/2023/5660481 (2023).
31. Lissea, T. S. et al. Paclitaxel-induced epithelial damage and ectopic MMP-13 expression promotes neurotoxicity in zebrafish. *Proc. Natl. Acad. Sci. USA* **113**(15), E2189–E2198. https://doi.org/10.1073/pnas.1525096113 (2016).
32. Heurtault, B., Saulnier, P., Pech, B., Proust, J. E. & Benoit, J. P. *Physico-chemical stability of colloidal lipid particles* (Elsevier, 2003). https://doi.org/10.1016/S0142-9612(03)00331-4.
33. Jarzynska, K., Gajewicz-Skretna, A., Ciura, K. & Puzyn, T. Predicting zeta potential of liposomes from their structure: A nano-QSPR model for DOPE, DC-Chol, DOTAP, and EPC formulations. *Comput. Struct. Biotechnol. J.* **25**, 3–8. https://doi.org/10.1016/j.csbj.2024.01.012 (2024).
34. O'Brien, G. S. et al. Coordinate development of skin cells and cutaneous sensory axons in zebrafish. *J. Comp. Neurol.* **520**(4), 816–831. https://doi.org/10.1002/cne.22791 (2012).
35. North, R. Y. et al. Electrophysiological and transcriptomic correlates of neuropathic pain in human dorsal root ganglion neurons. *Brain* **142**(5), 1215–1226. https://doi.org/10.1093/brain/awz063 (2019).
36. Hartung, J. E. et al. Nuclear factor-kappa B regulates pain and COMT expression in a rodent model of inflammation. *Brain Behav. Immun.* **50**, 196–202. https://doi.org/10.1016/j.bbi.2015.07.014 (2015).
37. Duggett, N. A. et al. Oxidative stress in the development, maintenance and resolution of paclitaxel-induced painful neuropathy. *Neuroscience* **333**, 13–26. https://doi.org/10.1016/j.neuroscience.2016.06.050 (2016).
38. Kimmel, C. B., Ballard, W. W., Kimmel, S. R., Ullmann, B. & Schilling, T. F. Stages of embryonic development of the zebrafish. *Dev. Dyn.* **203**(3), 253–310. https://doi.org/10.1002/aja.1002030302 (1995).
39. Zhen, Y. et al. Paclitaxel loading in cationic liposome vectors is enhanced by replacement of oleoyl with linoleoyl tails with distinct lipid shapes. *Sci. Rep.* https://doi.org/10.1038/s41598-021-86484-9 (2021).
40. Steffes, V. M. et al. Distinct solubility and cytotoxicity regimes of paclitaxel-loaded cationic liposomes at low and high drug content revealed by kinetic phase behavior and cancer cell viability studies. *Biomaterials* **145**, 242–255. https://doi.org/10.1016/j.biomaterials.2017.08.026 (2017).
41. Nöth, J. et al. Analysis of vascular disruption in zebrafish embryos as an endpoint to predict developmental toxicity. *Arch. Toxicol.* **98**(2), 537–549. https://doi.org/10.1007/s00204-023-03633-x (2024).
42. Bragato, C. et al. Biocompatibility analysis of bio-based and synthetic silica nanoparticles during early zebrafish development. *Int. J. Mol. Sci.* https://doi.org/10.3390/ijms25105530 (2024).
43. Bragato, C., Persico, A., Ferreres, G., Tzanov, T. & Mantecca, P. Exploring the effects of lignin nanoparticles in different zebrafish inflammatory models. *Int. J. Nanomed.* **19**, 7731–7750. https://doi.org/10.2147/IJN.S469813 (2024).
44. Livak, K. J. & Schmittgen, T. D. Analysis of relative gene expression data using real-time quantitative PCR and the $2^{-\Delta\Delta CT}$ method. *Methods* **25**(4), 402–408. https://doi.org/10.1006/meth.2001.1262 (2001).
45. Koch, C. M. et al. A beginner's guide to analysis of RNA sequencing data. *Am. J. Respir. Cell Mol. Biol.* **59**(2), 145–157. https://doi.org/10.1165/rcmb.2017-0430TR (2018).
46. Young, K. & Morrison, H. Quantifying microglia morphology from photomicrographs of immunohistochemistry prepared tissue using imagej. *J. Visual. Exper.* https://doi.org/10.3791/57648 (2018).
47. Fontenete, S. et al. FISHji: New ImageJ macros for the quantification of fluorescence in epifluorescence images. *Biochem. Eng. J.* **112**, 61–69. https://doi.org/10.1016/j.bej.2016.04.001 (2016).
48. Longair, M. H., Baker, D. A. & Armstrong, J. D. Simple neurite tracer: Open source software for reconstruction, visualization and analysis of neuronal processes. *Bioinformatics* **27**(17), 2453–2454. https://doi.org/10.1093/bioinformatics/btr390 (2011).

Acknowledgements

The authors thank Dr Krasimir Slanchev from the Max-Planck Institute for Biological Intelligence for providing the Tg(isl2b:GFP)zb7 zebrafish strain. The authors are grateful to Prof. Francesca Re and Prof. Gabriella Nicolini from the University of Milano-Bicocca for the precious help. Furthermore, the authors thank Prof. Sara Pellegrino, Pharmaceutical science department, University of Milan for the MSLP synthesis.

Author contributions

Conceptualization, C.B., and A.P.; methodology, C.B., A.P., and M.K.; investigation, C.B., A.P., and M.K.; formal analysis, C.B., A.P., L.M., and P.M.; resources, C.B., A.P., M.K., and P.M., writing—original draft, C.B.; writing—review and editing, C.B., M.K., A.P., L.M., and P.M.; funding acquisition, L.M., M.K., and C.B.; All authors have read and agreed to the published version of the manuscript.

Funding

This research was funded by the "Bando Bicocca Starting Grants – Edizione 2023" within the project ANTAGONISM—targeting breast cancer using functionalized liposomes (ID 2024-ATESP-0003/PER), funded by the University of Milano-Bicocca, Milan, Italy.

Declarations

Competing interests
The authors declare no competing interests.

Additional information
Supplementary Information The online version contains supplementary material available at https://doi.org/10.1038/s41598-025-00258-1.

Correspondence and requests for materials should be addressed to C.B.

Reprints and permissions information is available at www.nature.com/reprints.

Publisher's note Springer Nature remains neutral with regard to jurisdictional claims in published maps and institutional affiliations.